Progress in Understanding Multi-Scale Dynamics of Drift Wave Turbulence

Ö.D. Gürcan, **P.H. Diamond**, C.J. McDevitt, M.A. Malkov

Center for Astrophysics and Space Sciences and Department of Physics, UCSD, 9500 Gilman Drive, La Jolla, CA 92093-0424 USA

email contact of main author: pdiamond@ucsd.edu

Abstract. We report on progress in understanding the multi-scale dynamics of drift wave turbulence. Significant progress has been made on a) tearing mode and low-q resonance coupling to the inverse cascade in drift wave turbulence, b) the theory of turbulence spreading, c) the non-diffusive transport of toroidal momentum and d) L-H transition dynamics and the pedestal width. In this paper, special attention is focused on multi-scale convective cell and shear flow dynamics and ITB formation at low-q resonances.

1. Introduction

Multi-scale phenomena involving drift wave turbulence are ubiquitous in confined plasmas. One example of a multi-scale phenomenon involving drift wave turbulence which has received considerable attention in recent years is the problem of zonal flow dynamics and its impact on confinement [1]. In this paper, we report on recent progress in understanding the multi-scale dynamics of drift wave turbulence. In view of the length constraints imposed here, the focus of this paper is on convective cell shear flow dynamics and its role in internal transport barrier (ITB) formation at low-q resonances. However, we would like to remind the reader that we have recently made significant progress on tearing mode and resonant-q coupling to the inverse cascade in drift wave turbulence [2], the theory of turbulence spreading [3], the non-diffusive transport of toroidal momentum [4], and L-H transition dynamics - in particular an exact analytical solution of the minimal model of the L-H transition and a study of its implications for the width of the H-mode pedestal [5]. For details on any of these, the reader is directed to our recent publications cited above.

2. Electrostatic Convective Cells, Low-q Resonances and ITBs

Understanding of transport barrier formation in the vicinity of low-q rational surfaces remains a popular topic but an elusive goal [6]. Many candidate mechanisms have been proposed [7]. These include, but are not limited to: magnetic islands creating local, sharp gradients in profiles, sheared electric fields responding to magnetic topology changes or energetic particle dynamics, “rarefaction” of resonant surfaces and its effect on global (i.e. ballooning) modes [8], or ‘zonal flows’ forming at ‘profile corrugations’ near low-q resonances [9, 10]. Detailed GYRO simulation results [10] have been invoked to support the zonal flow and corrugation hypothesis, but these investigations left ample room for further analysis and theoretical work. In particular, the central question of *why zonal flows are linked to low-q resonances remains unanswered*. In this paper, we build upon our previous work on multi-scale interaction [2] to propose a simple model of how electrostatic convective cells trigger ITB formation *near*, but not *at*, low-q resonances in plasmas with weak magnetic shear. This model directly relates flow profile structure to the presence of low-q resonances.

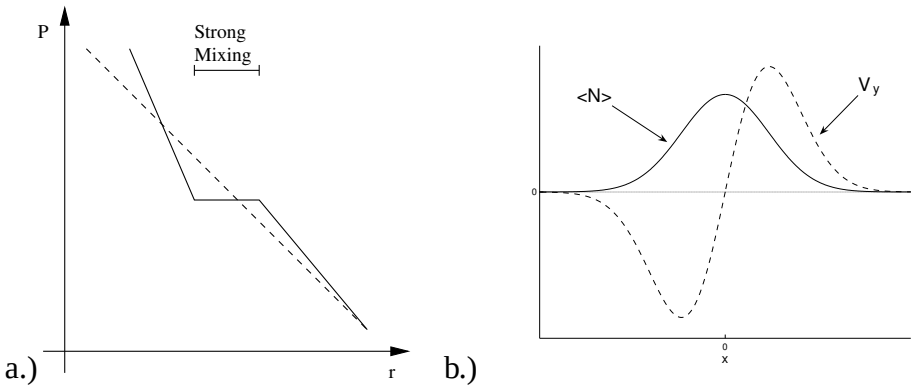

Figure 1: a.) Sketch of pressure profile in presence of vortex mode. Broken line corresponds to original pressure profile and the solid line corresponds to corrugated profile. b.) Profile of Reynolds stress driven flow (dotted) and fluctuation envelope (solid).

A major challenge to any model of ITB formation at low-q resonances is the need to simultaneously explain the dual experimental observations of:

a) a region of profile flattening (i.e. "corrugation") *at* the resonant surface, which is suggestive of strong, but localized, mixing or transport in that region,

b) the appearance of a transport barrier, due to strong $\mathbf{E} \times \mathbf{B}$ shear flow, in the region *nearby* the low-q resonance.

Of course, observations a) and b) are compatible, since strong localized mixing can induce the formation of $\mathbf{E} \times \mathbf{B}$ shear flows in the layer where ∇P and ∇n steepen immediately adjacent to the mixing zone (see Fig. (1a)). In addition, Reynolds stress driven shear flows are necessarily strongest in regions of large fluctuation intensity *gradient*, so a *local maximum* in the fluctuation intensity profile can result in the formation of a dipolar shear layer *around* the resonant-q (see Fig. (1b)). Considered together, all this suggests that the *fine structure of the turbulence intensity profile is the critical element linking shear flows to a low-q resonance*. Thus, in this paper we focus on the question of how low-q resonances 'structure' the turbulence and shear flow profiles in order to trigger ITB formation. Our central thesis is that electrostatic convective cells naturally form at low-q resonances, and locally flatten profiles at the resonance while they drive shear flows nearby. Two possible mechanisms for cell formation are examined, namely:

a) modulational instability-induced growth of a low m, n convective cell resonant at r_s, such that $q\left(r_s\right) = m/n$ [2]. Such cells naturally flatten profiles over their radial extent (so producing 'corrugations') while simultaneously driving flow shear which (initially) increases with $r - r_s$, and so is strongest away from the resonance. This scenario is especially pertinent to weak shear regimes.

b) strong coupling of the numerous radially co-located harmonics excited at a low-q resonance. In this scenario, nonlinear interaction of harmonics alters the underlying eigenmode structure, producing a robust, localized peak in the turbulence intensity. Intensity profile structure of this sort has long been observed in simulations of drift wave turbulence [11]. The locally peaked profile structure naturally drives a dipolar shear layer around, but not at, the resonant surface, as shown in Fig. (1b). This mechanism is not limited to regimes of weak magnetic shear.

We predict a power threshold for the onset of the flow in both cases. Also, in both cases the resulting shear flow acts to "trigger" an $\mathbf{E} \times \mathbf{B}$ transport bifurcation by a mechanism described previously [12].

2.1. Secondary Vortex Cell

The secondary vortex cell provides a physical mechanism which combines *both* local profile flattening *at* the resonant surface with profile steepening near it. The physical agent for this is a low-m secondary convective cell, driven by nonlocal transfer of energy from high-k, radially co-located drift waves. This structure is a finite m, n analogue of the zonal flow (which has $m = n = 0$), and is somewhat similar in concept to the idea of a "convective cell" originally proposed by Dawson and Sagdeev. These secondary cells are strongly localized near resonant surfaces, and damped by friction (as are zonal flows), field line bending, viscosity, Landau resonance, etc. They usually are of negligibly small width in normal shear regimes, but become broader and stronger in regimes of weak magnetic shear, which are characteristic of the regimes off-axis minimum q discharges we consider. Interestingly, results of GYRO simulations also indicate that profile corrugations are wider in weak shear than in normal shear [13, 10] regimes.

Much of the basic theory of the secondary electrostatic vortex cell is presented in Ref. [2]. A minimal description of the structure requires two elements, namely a dynamical model of the large scales which incorporates stresses induced by small scales and a model of the turbulence and how it responds to large scale cellular flow.

a) Dynamical Model of the Large Scales

The simplest example is reduced MHD, including vorticity advection by small scales which produces the fluctuation Reynolds stress, i.e.

$$\frac{\partial}{\partial t}\psi = v_A \frac{\partial}{\partial z}\phi + \eta \nabla_\perp^2 \psi \ , \tag{1a}$$

$$\left(\frac{\partial}{\partial t} + \gamma_d\right) \nabla_\perp^2 \phi = v_A \frac{\partial}{\partial z}\nabla_\perp^2 \psi + \nu_c \nabla_\perp^2 \nabla_\perp^2 \phi - \frac{c}{B_0}\left\langle (\hat{\mathbf{z}} \times \nabla\tilde{\phi}) \cdot \nabla \nabla_\perp^2 \tilde{\phi} \right\rangle \ , \tag{1b}$$

b) Model of the Turbulence

Here, wave kinetics [1] provides the simplest framework, and allows us to evolve the mean intensity of the drift wave turbulence according to

$$\frac{\partial \langle N \rangle}{\partial t} = \frac{\partial}{\partial k_x}\left(D_k \frac{\partial \langle N \rangle}{\partial k_x}\right) + \frac{\partial}{\partial x}\left(D_x \frac{\partial \langle N \rangle}{\partial x}\right) + \gamma_k \langle N \rangle - \Delta\omega_k \langle N \rangle^2 \ , \tag{2}$$

The notation in Eqns. (1,2) is standard, and is discussed extensively in Ref. [2]. $\langle N \rangle$ is the averaged wave quanta density, which evolves by k-diffusion due to flow shear, spatial diffusion due to flow advection, linear growth and local interaction, γ_d is the scale-independent flow damping due to trapped-untrapped friction, and ν_c is the collisional viscosity. Here,

$$D_k = k_y^2 \sum_q R(k,q)\, q_x^4 \left|\phi_q\right|^2 , \qquad D_x = \sum_q R(k,q)\, q_y^2 \left|\phi_q\right|^2 \ . \tag{3}$$

Also, $R(k,q) = \gamma_k / \left[\gamma_k^2 + (\omega_q - \mathbf{v}_{gr}\cdot\mathbf{q})^2\right]$ is the resonance function controlling the interaction time between drift wave and cell.

For $\Delta' > 0$, Eqns. (1,2) describe a tearing mode, modified by coupling to drift wave stresses and the associated inverse cascade, as discussed in Ref. [2]. For $\Delta' \ll 0$, the physical entity described by Eqns. (1,2) is a localized low-m electrostatic vortex cell, which is a secondary structure excited by the ambient turbulence. In this limit, one can follow the two-scale, adiabatic renormalization procedure used in Ref. [2] to derive a Fourier transformed evolution equation for the vortex cell

$$\frac{v_A^2 q_y^2}{\eta L_s^2}\frac{d^2\phi_q}{dq_x^2} = \left[\left(\nu_c + \nu_T(q_x)\right)q_x^2 + \gamma_d + \frac{\partial}{\partial t}\right] q_x^2\phi_q \,, \tag{4a}$$

$$\nu_T = c_s^2 \sum_k R(k,q)\,\frac{\rho_s^2 k_y^2}{\left(1+\rho_s^2 k_\perp^2\right)^2} k_x \frac{\partial\langle N\rangle}{\partial k_x} \,. \tag{4b}$$

Here again, the notation is standard (see Refs. [1, 2] for details). For $\partial\langle N\rangle/\partial k_x < 0$ (always true for drift wave turbulence), $\nu_T < 0$, so the effective turbulent viscosity is *negative*, which corresponds to pumping of large scales by small scales as in an inverse cascade. Also, keep in mind that the effects of turbulent vorticity advection will no longer appear as a simple viscosity for large q_x, on account of the intrinsic q_x-scaling of $R(\mathbf{k},\mathbf{q})$. Eqn. (4) also takes $q_\parallel = q_y(x/L_s)$, where $x = r - r_{m,n}$ and $r_{m,n}$ is the location of the m,n rational surface.

Eqns. (2) and (3) constitute a closed, self-consistent description of the dynamics of a low-m, electrostatic vortical cell evolving in the presence of drift wave turbulence. Unlike the zonal flow, the resonant finite-m vortex cell drives radial transport (since $\tilde{v}_r \neq 0$) and also is damped by field line bending (or, more generally, Landau damping) and collisional viscosity, as well as by trapped-untrapped friction. Thus, the vortex cell is more strongly damped than the zonal flow, which is (linearly) damped only by collisional friction. The width of the cell is determined by the interplay between field line bending (i.e. magnetic shear!) and viscosity. Thus, we see that finite m, n vortex cells are alway tightly localized at $\mathbf{k}\cdot\mathbf{B} = 0$ resonances and more damped than zonal flows, and so are usually subdominant to zonal flows. However, in the weak shear regimes characteristic of off-axis minimum q plasmas, they can be considerably broader and less damped than in normal shear regimes, and so are an attractive candidate for explaining the simultaneous appearance of *neighboring regions of flattening and shearing*, as noted earlier. Of course, zonal flows, which have $\tilde{v}_r = 0$, cannot *themselves produce* flat spots in profiles at resonances. We also note that GYRO simulations indicate that corrugations are radially wider in weak shear regimes, consistent with our expectations for the secondary vortex cell [13, 10].

Eqn. (3) may be solved as an eigenvalue problem in order to determine the flow shear profiles and saturated turbulence levels of the coupled drift wave-vortex cell system. Here, the drift wave turbulence intensity is the "eigenvalue" and the cell flow profile is the "eigenfunction". To this end, it is convenient to write $|\nu_T(q_x)|$ as

$$|\nu_T(q_x)| \approx c_s^2 \frac{\gamma_k}{\gamma_k^2 + (q_x v_{gr})^2}\langle N\rangle \approx \frac{4D_{GB}}{1+(4\rho_s q_x)^2}\frac{\langle N\rangle}{N_{ML}} \,, \tag{5}$$

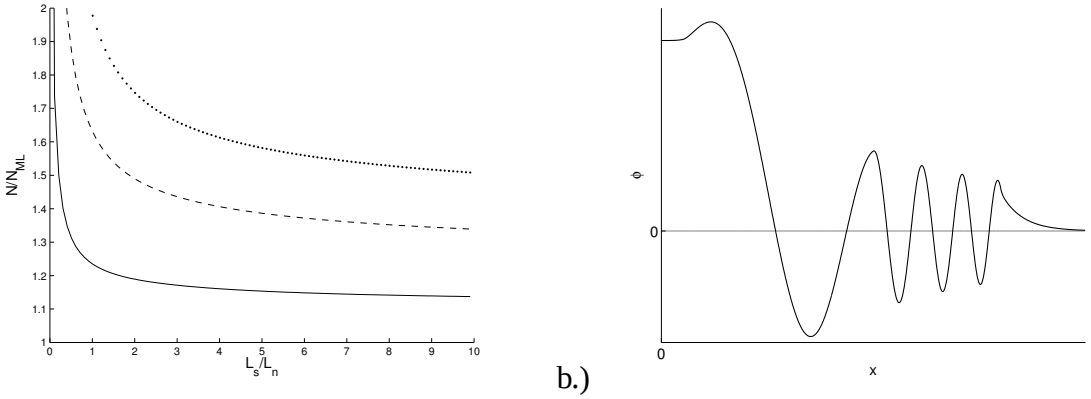

a.) b.)

Figure 2: a.) Saturated intensity of drift wave turbulence for three values of viscosity for the parameters $\gamma_d/\gamma_k = 1$, $\eta/D_{GB} = 1/10$, $\beta = 1/20$, $m = 2$, and $\rho^* = .01$. The solid curve corresponds to $\nu_c/D_{GB} = .01$, the broken curve to $\nu_c/D_{GB} = .05$, and the last curve to $\nu_c/D_{GB} = .1$. b.) Sketch of radial potential profile of the vortex cell.

Here $v_{gr}/\gamma_k \approx 4v_e^*/\omega_e^* \approx 4\rho_s$, $N_{ML} = (\rho_s/L_n)^2$, and $D_{GB} = (\rho_s/L_n)\, c_s\rho_s$ is the usual gyro Bohm diffusivity. A *lengthy* calculation than gives the eigenvalue condition:

$$\frac{2}{3}\sqrt{\frac{\nu_c}{|\nu_T(0)|}}\left(\frac{\Delta x}{\rho_s}\right)^3\left\{\sqrt{z_c+\zeta}\left[\zeta \mathrm{E}\left(\sqrt{\frac{2z_c}{z_c+\zeta}}\right)-(\zeta-z_c)\,\mathrm{K}\left(\sqrt{\frac{2z_c}{z_c+\zeta}}\right)\right]\right\}=\frac{\pi}{2}+\delta\,. \tag{6}$$

Here $N = \langle N\rangle/N_{ML}$, $\hat{\nu}_c = \nu_c/D_{GB}$, $\Gamma = \gamma_d/\gamma_k$, $\zeta \equiv (1/8)\left((N-\Gamma)/\hat{\nu}_c - 1/4\right) + 1/16$, $z_c = (1/8)\sqrt{\left((N-\Gamma)/\hat{\nu}_c - 1/4\right)^2 - \Gamma/\hat{\nu}_c}$, and δ is a small shift neglected hereafter. E and K are complete elliptic integrals. Expanding to first order in $\hat{\nu}_c$ (note $\hat{\nu}_c \ll 1$, here), we derive the 'eigenvalue' relation for the saturated turbulence level, namely:

$$N \approx \Gamma + \left(\frac{3\pi}{2}\frac{1}{1-\epsilon}\right)^{2/3}\frac{\nu_c^{2/3}}{\eta^{1/3}}\left(\frac{v_A q_y}{L_s}\right)^{2/3}\frac{1}{\gamma_k}\,, \tag{7a}$$

$$\epsilon \equiv \frac{3}{4}\alpha\left(\ln\left(\frac{16}{\alpha}\right)-\frac{N-2\Gamma}{N-\Gamma}\right), \quad \alpha \equiv \frac{1}{4}\frac{N}{(N-\Gamma)^2}\hat{\nu}_c\,. \tag{7b}$$

Eqn. (7) clearly shows the dependence of turbulence levels on both friction and line bending. Also, even though $\nu_c/D_{GB} \ll 1$, terms of $O(\alpha)$ can be significant, on account of the $(N-\Gamma)^{-2}$ factors. This surprisingly strong dependence of N on collisional viscosity and field line bending can be understood by considering the synergy between these two effects. Stronger field line bending (i.e. from strong magnetic shear) localizes the cell more sharply, so in turn the rapid variation of the cell eigenfunction becomes more sensitive to viscous damping. In Fig. (2a), the saturated value of N (i.e. eigenvalue) is plotted vs. L_s/L_n for three different values of viscosity. The sensitivity to magnetic shear is evident, supporting the assertion that low-m vortex cells are most active in regimes of weak magnetic shear.

Regarding the vortex cell flow structure (i.e. the eigenfunction), asymptotic analysis of Eqn. (4) (with ν_T taken independent of q_x for convenience) yields an approximate expression for the potential profile of the vortex cell, which is

$$\phi(x) \sim \frac{1}{x^{3/4}} \exp\left(i\frac{2}{3}\left(\frac{x}{\Delta x}\right)^{3/2}\right) . \tag{8}$$

An asymptotic calculation of the vortex cell potential profile is shown in Fig. (2b). The width of the cell, which sets the scale of the flat spot or corrugation over which profiles are mixed, scales as $\Delta x \equiv \left(\left|\nu_T(0)\right|\eta\right)^{1/6}\left(L_s/\left(v_A q_y\right)\right)^{1/3}$, and increases with L_s. Interestingly, the *strength of the cell's flow shear* scales as $\left|v_y'\right| \sim x^{1/4}$, and so *grows with distance from the resonant surface*. This is evident in Fig (2b), as well. These results suggest that the vortex cell will suppress turbulence *nearby, but off,* the resonant surface more strongly than it will affect fluctuations *at* the resonant surface. This appears consistent with the dual observations of persistent transport or mixing *at* the surface (needed for the local flat spot) along with flow shear suppression of turbulence *nearby* the surface. We also note that the resulting peaked fluctuation profiles can also drive $m = 0$, $n = 0$ shear flows via the Reynolds stress. In that case, the *flow drive* is *strongest* in the region of *largest intensity gradient*, which sits *away* from the resonant surface, as sketched in Fig. (2b). Such flows will, of course, also enhance the formation of ITBs.

We add in passing that the tendency to form Reynolds stress driven shear layers at the periphery of regions of mixing by cell advection is quite consistent with the well known, generic process of homogenization of potential vorticity in over-turning convective cells [14]. In this process, shear flow and diffusion combine to expel potential vorticity from the cell, thus creating sharp vorticity gradients at the cellular boundary. These thin regions of sharp vorticity gradient are the location of the 'transport barriers' at the boundary of the cell. Thus, we see that the coupling of the two processes of steepening and flattening is *generic* to systems for which vorticity advection is an important element of the dynamics.

The eigenvalue condition of N given by Eqn. (7a) implies that a critical drift wave fluctuation level is required to trigger cell formation. The critical level is simply that fluctuation intensity which is required for the Reynolds stress to drive the cell against friction, line bending, etc. This, in turn, translates into a power threshold. Using a standard, simple model of ITG turbulence, we can write the heat flux in terms of N as

$$Q = q_r = -\chi_{\text{crit}}\frac{\partial T_i}{\partial r} \approx v_{th} T_i \eta_i \epsilon_T^{-1/2} \tau^2 N . \tag{9a}$$

Applying power balance gives $P_{\text{in}} \sim R r_b v_{th} T_i \eta_i \epsilon_T^{-1/2} \tau^2 N_{crit}$, where

$$N_{\text{crit}} \approx \Gamma + \left(\frac{\frac{3\pi}{2}+\delta}{1-\epsilon}\right)^{2/3} \frac{\nu_c^{2/3}}{\eta^{1/3}} \left(\frac{v_A q_y}{L_s}\right)^{2/3} \frac{1}{\gamma_k} . \tag{9b}$$

Here r_b is the radius at which the barrier is located and the rest of the notation is standard. Not surprisingly, the power threshold increases with increasing collisional friction, magnetic shear strength and viscosity. Note also that the strength of the total flow damping, rather than the oft-invoked but naive γ_L vs. $\omega_{\mathbf{E}\times\mathbf{B}}$ criterion, is what sets the threshold for vortex cell formation.

2.2. Strong Coupling of Resonant Harmonics

A second mechanism for producing local fluctuation intensity maxima and profile corrugations works by strong nonlinear coupling of the many harmonics which are naturally co-located at a

low-q resonance. In this mechanism, coupling of harmonics, rather than secondary instability, leads to formation of an electrostatic convective cell at the low-q resonance. Harmonic coupling was extensively studied in the context of drift wave turbulence in Ref. [11], albeit for an extremely simple model. That study revealed that the spatial profile of fluctuation intensity develops local peaks at low order rationals on account of the alterations (of both the eigenmode structure and how it couples to dissipation) which are induced by the strong, localized, nonlinear interaction of the many harmonics. Spatial intensity profile peaks were predicted and observed to form such 'single helicity structures' when the strength of interaction between the resonant harmonics exceeded the strength of multiple helicity interaction with neighboring modes. Since formation of local intensity maxima were observed to occur in normal q profiles, it seems reasonable to speculate that the rarefaction of resonant surfaces around a low-q resonance caused by weak magnetic shear (characteristic of off-axis minimum q discharges) will only *enhance* the tendency to form peaks in the turbulence intensity profile.

The analysis of Ref. [11] did not address the dynamics of a self-generated (i.e. Reynolds stress driven) flow and its interaction with the local intensity maximum. Here we extend that analysis to determine the profile of the self-generated flow which coexists with the intensity maximum, as well as the threshold for growth of the self-generated flow. The fluctuation induced Reynolds stress can be straightforwardly computed using the nonlinear mode structure given in Ref. [11]. For the case of a narrow shear layer, the resulting stationary shear flow profile is

$$\frac{v_y}{v_y'\left(0\right)} = \frac{\nu_i L_s^2}{c_s}\frac{\omega_{ci}}{\gamma_d}\left(\rho_s^2\alpha_h\right)^2\frac{x}{\rho_s}\exp\left(-\alpha_h x^2\right)\int\frac{dk_y}{k_0}\left(1+\rho_s^2k_y^2\right)\left|\frac{\tilde{n}_k}{n_0}\right|^2 \quad , \tag{10}$$

Here the notation is that of Ref. [11], $\left(\alpha_h\right)^{-1/2}$ is the intensity profile width. Note that the resulting shear layer is dipolar, localized to an intensity profile width of $\left(\alpha_h\right)^{-1/2}$, and stronger for weak magnetic shear. The critical intensity for triggering growth of the flow is given by

$$\int\frac{dk_y}{k_0}\left(1+\rho_s^2k_y^2\right)\left|\frac{\tilde{n}_k}{n_0}\right|^2 = \left(\frac{1}{\rho_s^2\alpha_h}\right)\left(\frac{1}{\alpha_h L_s^2}\right)\left(\frac{\gamma_d}{\nu_i}\right) \quad . \tag{11}$$

Obviously, the critical intensity level can easily be converted to a power threshold by the procedure outlined in Section 2.1. It is not surprising that the critical power increases with the flow damping γ_d while decreasing for weaker magnetic shear. The structure of the single helicity intensity profile and flow profile are shown in Fig. (1b).

3. Scenario for ITB Formation

As the last element of this discussion, we remind the reader that the Reynolds stress driven shear flow discussed here will act as a *trigger* for ITB formation, which occurs in *two* stages [12]. In the first stage, growth of sheared flow begins when $P \gtrsim P_{crit}$, resulting in a moderate reduction in fluctuation level, and thus a steepening in the local pressure and toroidal velocity gradients. In the second stage, the electric field shear from the steepened ∇P and v_ϕ is sufficient to severely quench or extinguish the fluctuations, so that a recognizable ITB forms. However, the quench of fluctuations means that the Reynolds stress driven flow damps away, so the dominant contributors to E_r' in the "end state" ITB are ∇P and v_ϕ. This evolutionary sequence is illustrated in Fig. (1) of Ref. [12]. The role of Reynolds stress driven flows as a trigger is

suggested by the observations that at high power, ITBs can form in the absence of resonant-q, and that the incidence of ITB formation is sensitive to the mean electric field shear, which can be changed by varying the mixture of co and counter injection [15].

4. Conclusion

This paper has discussed the application of recent advances in our understanding of multi-scale interaction processes in drift wave turbulence to the problem of understanding the fluctuation intensity profile structure near low-q resonances and its implications for the mechanism by which ITBs are triggered there. Two mechanisms for generation of localized electrostatic convective cells at the resonant surface are discussed. One involves low-m secondary structure, the other is based on strong coupling of resonant harmonics. Which of these two mechanisms is dominant is a quantitative question, the answer to which requires a detailed, case-by-case analysis. We emphasize, too, that the two mechanisms are *not* mutually exclusive and *can* work in synergy. In both cases, the models analyzed are extremely simple, so much further work is required. Trapped ion modifications may be particularly important for low collisionality regimes, and should be explored carefully.

5. Acknowledgments

We thank K. Burrell, X. Garbet and T.S. Hahm for helpful discussions. This research was supported by DOE Grant DE-FG02-04ER54738.

References

[1] DIAMOND, P. H. et al., Plasma Phys. Control. Fusion **47** (2005) R35.

[2] MCDEVITT, C. J. et al., Phys. Plasmas **13** (2006) 032302.

[3] GURCAN, O. D. et al., Phys. Rev. Lett. **97** (2006) 024502.

[4] GURCAN, O. D. et al., submitted to PoP 2006, and references therein.

[5] MALKOV, M. et al., submitted to PoP 2006.

[6] CHALLIS, C. D. et al., Plasma Phys. Control. Fusion **47** (2005) R35.

[7] CONNOR, J. W. et al., Nucl. Fusion **44** (2004) R1.

[8] GARBET, X. et al., Phys. Plasmas **8** (2001) 2793.

[9] AUSTIN, M. E. et al., Phys. Plasmas **13** (2006) 082502.

[10] WALTZ, R. E. et al., Phys. Plasmas **13** (2006) 052301.

[11] CARRERAS, B. A. et al., Phys. Fluids B **4** (1992) 3115.

[12] DIAMOND, P. H. et al., Proceedings of 15th IAEA Conference **3** (1996) 323.

[13] WALTZ, R. E. et al., Nucl. Fusion **45** (2005) 741.

[14] RHINES, P. B. et al., J. Fluid Mech. **122** (1982) 347.

[15] BURRELL, K., Private Communication, 2006.